Available online at www.CivileJournal.org

Civil Engineering Journal

(E-ISSN: 2476-3055; ISSN: 2676-6957)

Vol. 7, No. 01, January, 2021

Analytical and Numerical Model of Aluminum Alloy Swaging Ring Design to Study the Effect on the Sealing for Piping Systems

Ahmet Atak [1*]

[1] *TUSAŞ-Kazan Vocational School, Gazi University, Aydın Mahallesi, Aydın Küme Evleri, 1.Cadde, No: 79/A, Kahramankazan, Ankara, Turkey.*

Received 01 September 2020; Revised 05 December 2020; Accepted 19 December 2020; Published 01 January 2021

Abstract

In various fields of engineering, the assembly and repair of hydraulic installations are accomplished by joining the pipes. In such applications, the ring swaging method is used to connect the fittings to the pipes by means of a hydraulic hand tool. The basis to develop a swaging tool relies on the knowledge of the design parameter that influence plastic deformation of the swaging ring. In addition to build control over the design parameters, it is necessary to join pipes under severe conditions such as cryogenic vacuum and constrained space which require an intact sealing. In this study, the effect of swaging ring designs on sealing and strength has been examined and different swaging methods have been investigated by finite element modeling methods. Based on the obtained results, the analysis methodology of ring swaging and the characteristic impact of swaging ring design on the sealing of pipe connection are shown. The prime novelty of the study is to report the impact of swaging ring design and geometry on sealing efficiency of the pipe connection. The results of the study open new avenues for the development of efficient tools for designing swaging rings.

Keywords: Joining in Piping; Sleeve Design; Swaging Ring; Sleeve Swaging Method; Pipe Connection.

1. Introduction

The structural engineers face many challenges to design and build the budget-consuming projects with safety and durability. The heavy loads may damage the piping structures or disturb their normal operation whenever their magnitudes reach the threshold limit of the mechanical strength [1, 2]. Predominantly, the structural engineers perform three-dimensional (3D) finite element analyses to investigate the behavior of the buried pipe that are exposed to strike-slip fault movement in dry and partially saturated sand [2]. The theoretical studies report the potential zones which are dangerous in the piping connection of column-type devices. Such numerical studies can be used to make decisions to improve the safety of hazardous regions in the production facilities corresponding to the oil and gas industry, at the design, operation and diagnostic stages [3-5]. Pertaining to joining in structural engineering and mechanical handling, the design and analysis engineers recommend to specify the mechanical closure and fatigue conditions that depend on the swage parameter and material utilized in swage rings [6]. In some loading cases, to obtain more realistic results from the design analysis of structural systems, it is necessary to determine the suitable fastener stiffness values in their connections [7]. It is necessary to propose an analytical or numerical method that is useful to the practicing engineers during the design of pipe connections and structural analysis [8, 9]. The most critical part of a piping is their connections, with each other or with the equipments. Piping solutions using non-welded connections and cold bent

* Corresponding author: ahmetatak@gazi.edu.tr

http://dx.doi.org/10.28991/cej-2021-03091641

methods offer significant value owing to the reductions in fabrication and commission time, while improving the workplace safety. The benefits of non-welded piping technology include easy preparation and reduced inspection time and a safer work environment [10].

Among the different methods used to join tubes, one of the most efficient is by rotary swaging. In this method the rotation energy is converted to thermal friction energy and the ring is swaged on the pipe which results in almost 100 % sealing [11, 12]. Swaging as a joining method is currently used in the most crucial industries including military, automotive, and medicine. Within the military industry, swaging is used to form items such as gun barrels and anti-tank rocket tips. Many automobile components, including the assemblies for emergency brake cables, steering components, and drive shafts, are formed using swaging machines. In medicine; hypodermic needles, catheter band assemblies, and optical instruments are a few of the many medical products that undergo swaging. In renewable energy, cartridge heaters, superconducting material, and zirconium rod can be expertly machined using swaging machines. In aerospace industry, the swaging process assures the production of high-quality control rods, wire rope cable assemblies, and fluid transfer tubing [13]. Further, swaged pipes have been increasingly used for offshore pipeline system. Predominantly, swaging tubes and pipes are made of steel.

The process is also established for other structural materials such as stainless steels, aluminum, and titanium alloys. The swaged end joint is fabricated by a cold deformation process on the outer pipe which is subsequently welded to the inner pipe. The pipe-in-pipe system has excellent thermal insulation characteristics [14]. However, the accounted literature review shows the importance of the connection parts of a structural pipe system for the structural design engineers. Normal installation of piping systems are designed at <16 bars and connections are designed with removable flanges or screws. In screw compression connections, both the connection and sealing are provided by swaging a conical metal or hard rubber intermediate element between the screw and the nut [15]. Piping of hydraulic systems operating under high pressure are usually made with rubber pipes and fittings that are connected to the ends of the pipes by the sleeve swaging method. Plastic pipes and fittings are subjected to pressure tests at a pressure of 1.5 times the working pressure and under burst pressure. In the aviation field, hydraulic facility pipes are made with aluminum, stainless steel, or rubber pipes. Their sealing performance is evaluated by vibration tests at conditions closer to the threshold levels [15].

Most studies have used a simulation software like Forge 2D, to determine the characteristics of the forging process and the studies were performed to find the best swaging parameter, such as friction coefficient, during material flow, or the best suitable swaging process [9, 12, 16]. To show the methodology of this study, we prepared the flowchart shown in Figure 1.

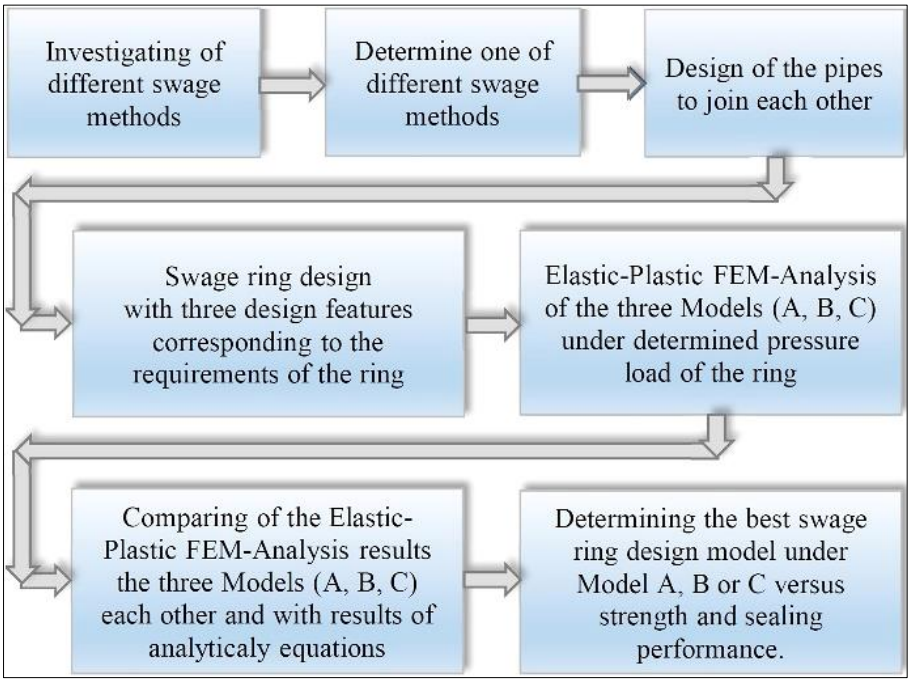

Figure 1. Flowchart of the methodology

There are limited studies which report the design and analysis of ring swaging pipe connection [17]. Figure 2 shows a schematic of swaging type A, wherein both the direct connection of two pipes and the connection of the fittings are done by the design of swaging ring (sleeve). Based on the nature of the pipes to be connected, different swaging parameters are determined. These welded connections are expected to withstand more pressures than the pipe. The

design of the swaging ring greatly affects the mechanical bearing properties and sealing of the connection. The tightened area is slightly inclined and wavy in the axial direction, as seen in Figure 2, making the sliding of the pipe difficult when pulled in the axial direction. Similarly, when the swaging ring is designed with circumferential waves, it is difficult for the pipe to turn inside the ring. In addition, two internal circumferential grooves are designed to place an O-Ring into the ring, providing further sealing.

Figure 2 also shows the sectional view of swaging type A. The swaging ring is tightened in two steps by applying pressure to the first pipe from the right and then to the second pipe from the left radially to cause plastic deformation.

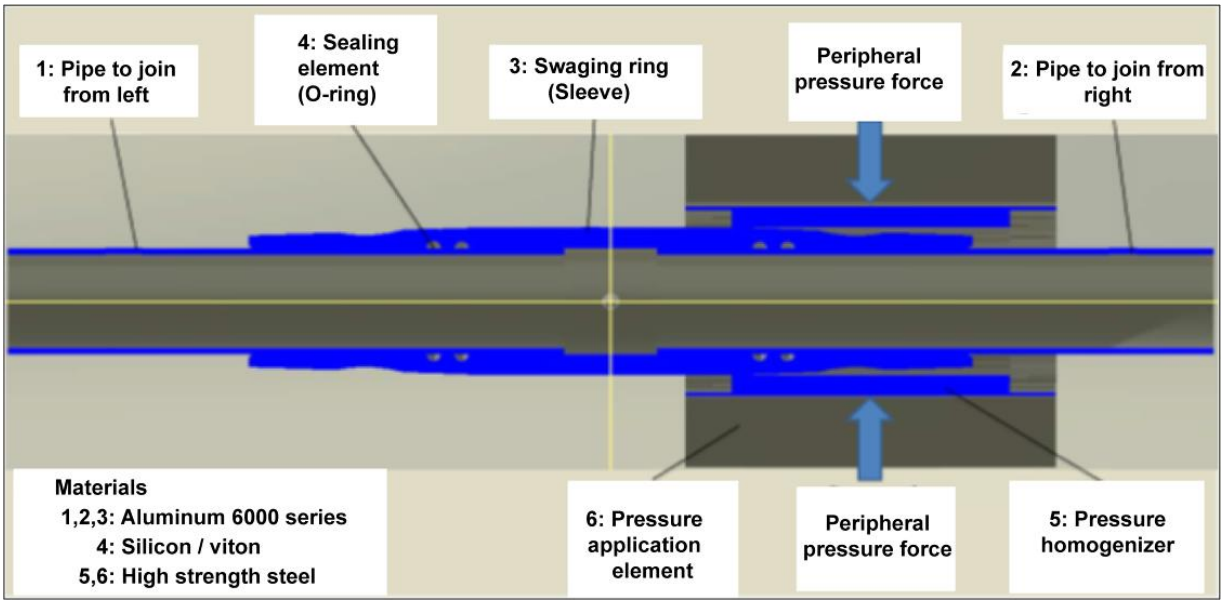

Figure 2. Swaging type A; Radial swaging elements with pressure homogenizer

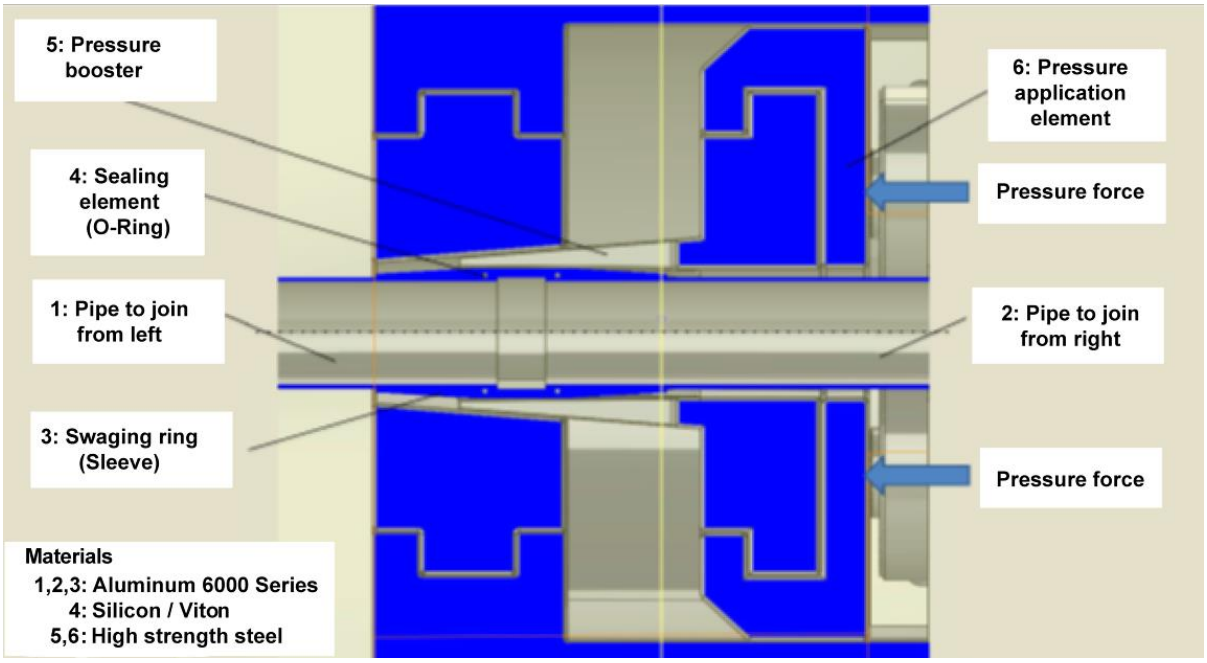

Figure 3. Swaging type B; Radial swaging elements with axial pressure and pressure booster

Figure 3 shows the sectional view of swaging type B. The swaging ring is tightened in two steps by applying pressure to the first pipe from the right and then to the second pipe from the left axially and radially to cause plastic deformation by a pressure booster wedge member. Figure 4 shows the sectional view of swaging type C. The swaging ring is tightened in a single step by applying pressure to the first pipe from the right and then to the second pipe from the left radially with the help of two riser wedge rings from right and left to cause plastic deformation. The two riser rings remain non-detachable on the swaging ring. In all the three configurations, the pipes and the middle part of the ring are exposed to pressure load that does not exceed elastic loading. When pipes are of different materials, different swaging parameters from right and left and different riser ring designs must be applied.

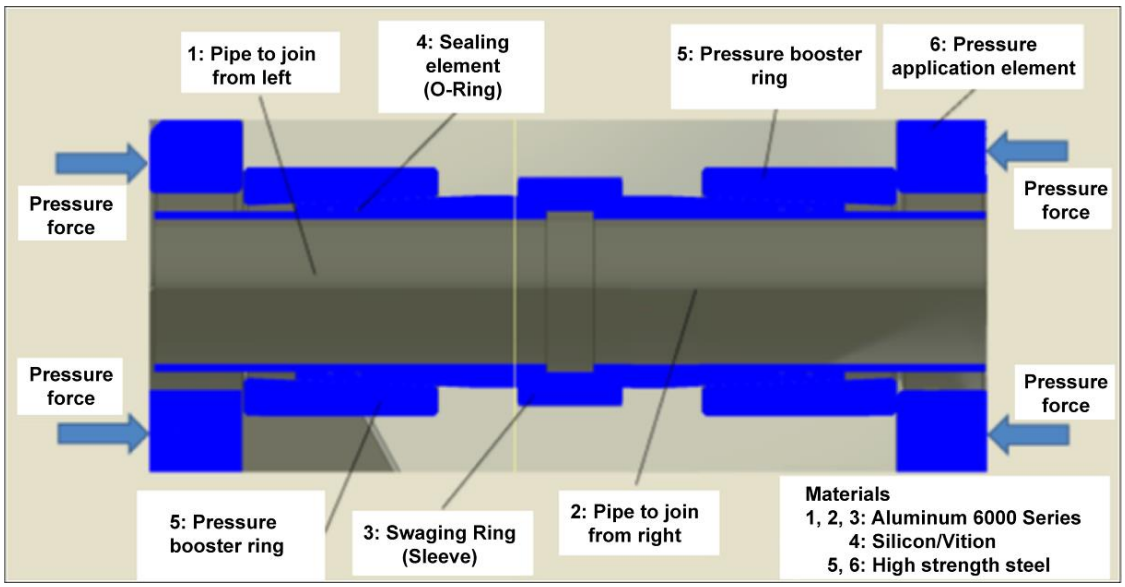

Figure 4. Swaging type C; radial swaging by tightly compressing the pressure booster (Wedge) ring to the swaging ring by axial pressure force

In this study, the swaging ring as shown in Figure 7 that does not show leakage under high or low pressures were swaged with method swaging type A. The joining of the two aluminum pipes is modeled and analyzed by analytical and numerical methods. Different designs of the aluminum alloy swaging ring is made and numerical solutions are obtained using the finite element method (FEM). Due to the nature of the method, swaging ring and pipes that are joined together and which may have different materials are subjected to elastic-plastic deformations. Therefore, the numerical solution is realized by a non-linear method [18]. Besides, since both the plastic deformation of the material and the friction contact between the elements occur, the solution is again inevitable by the non-linear method [19]. The non-linear numerical solution of the model is obtained using FEM [20]. Different swaging ring designs are analyzed and compared, and the connection has been improved by optimizing the swaging ring designs. The numerical method proposed in this study is useful for practicing engineers to comprehend the rational design of pipe connections in detail which would aid in designing and structural analysis.

2. Analytical Design of Swaging Ring

The working principle of swaging ring relies on its mechanical-elastic deformation under external pressure load. It also involves subjecting the inner connection pipe to the elastic-plastic deformation as shown in Figure 5.

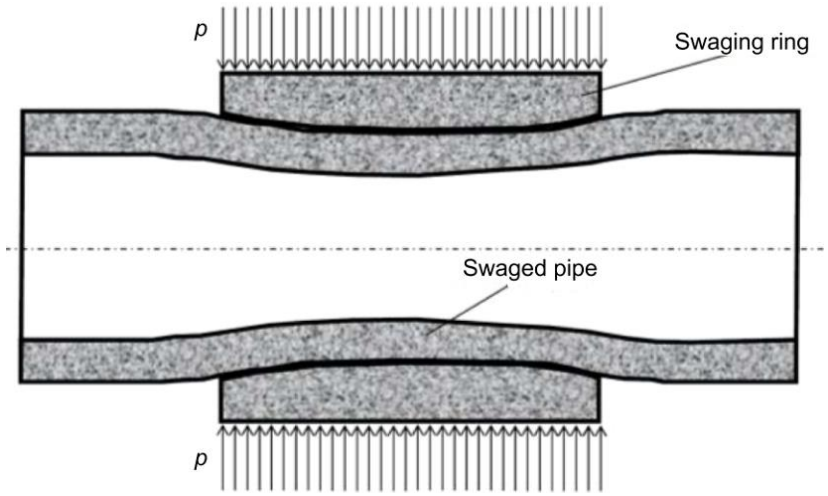

Figure 5. Swaging principle with swaging ring (sleeve)

Circumferential (tangential) and centrifugal (radial) tensions occur in the pipe tightened under external pressure. The centrifugal tension is equal to the pressure applied on the pressure surface which vanishes on the other inner surface. Since the ratio of the inner radius of the pipe to its thickness, matches with that of a thin pipe, in the range, $r_i/s > 5$, calculations are made according to the mean radius and very small variation in thickness are ignored [21]. Based on this assumption, the centrifugal tension is given by Equation 1:

$$\sigma_r = \frac{p}{2};\ s \ll r_m \quad (1)$$

Where: p: Pressure applied (MPa), d_a: Outer diameter of the pipe (mm), s: Pipe thickness (mm), $r_m = \frac{d_a - s}{2}$: Medium radius of the pipe (mm).

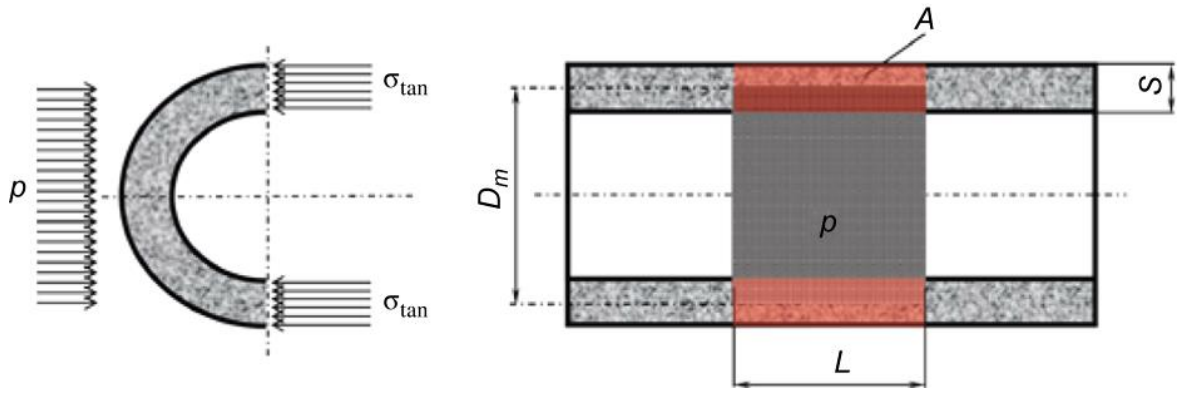

Figure 6. Circumferential (tangential) tension caused by pressure swaging

Figure 6 shows the circumferential tension σ_{tan} and other parameters occurring under the pressure applied on the pipe. Equation 2 is constituted in accordance with the principle of equality of forces in the horizontal direction:

$$\sigma_{tan} A = pD_m L \rightarrow \sigma_{tan} 2sL = pD_m L \rightarrow \sigma_{tan} = \frac{pD_m L}{2sL} \rightarrow \sigma_{tan} = p\frac{r_m}{s} \quad (2)$$

Where: σ_{tan}: Circumferential tension (MPa), p: Pressure applied (MPa), D_m: Medium diameter of the pipe (mm), s: Pipe thickness (mm), $r_m = \frac{D_m}{2} = \frac{d_a - s}{2}$: Medium radius of the pipe (mm).

Thus, when the equivalent tension is geometrically collected, it is found as given in Equation 3:

$$\sigma_E = \sqrt{{\sigma_{tan}}^2 + {\sigma_r}^2 - \sigma_{tan}\sigma_r} \rightarrow \sigma_E = \sqrt{\left(p\frac{r_m}{s}\right)^2 + \left(\frac{p}{2}\right)^2 - p\frac{r_m}{s}\frac{p}{2}} \rightarrow \sigma_E = p\sqrt{\left(\frac{r_m}{s}\right)^2 + \frac{1}{4} - \frac{r_m}{2s}} \quad (3)$$

Since h, a minimum degree of yield tension, is incident on the pipe, the least required minimum pressure is found by Equation 4:

$$p_{min} = \frac{R_{p0,2}}{\sqrt{\left(\frac{r_m}{s}\right)^2 + \frac{1}{4} - \frac{r_m}{2s}}} \quad (4)$$

Where: p_{min}: Required minimum pressure (MPa), $R_{p0,2}$: Yield tension (MPa).

Example: Swaging ring: R-29,4x2- 6061-T6;

Yield value: $R_{p0,2} = 240$ MPa.

$\rightarrow r_{m,a} = \frac{d_a - s}{2} = \frac{29.4-2}{2}$ mm = 13.7 mm; Medium radius of the swaging ring.

$\rightarrow p_{min,a} = \frac{240\ \text{Mpa}}{\sqrt{(\frac{13.7}{2})^2 + \frac{1}{4} - \frac{13.7}{2 \cdot 2}}} = 33{,}7$ MPa $= 337$ bar

Inner Pipe: R-25,4x0,75- 6061-T6;

Yield value: $R_{p0,2} = 240$ MPa

$\rightarrow r_{m,i} = \frac{d_{a,i} - s_i}{2} = \frac{25.4-0.75}{2}$ mm = 12.325 mm inner pipe medium radius.

$$\rightarrow p_{min,i} = \frac{240\ MPa}{\sqrt{\left(\frac{12{,}325}{2}\right)^2 + \frac{1}{4} - \frac{12.325}{2 \cdot 0.75}}} = 14{,}8\ MPa = 148\ bar$$

Total required minimum pressure: $p_{min} = p_{min,a} + p_{min,i} = 33.7$ MPa $+ 14.8$ MPa $= 48.5$ MPa.

In order to form both elastic and permanent plastic deflection in the tightened pipes, it is recommended to apply over 30% of the minimum pressure to the swaging ring. Example: $p = 1.3, p_{min} = 1.3 \cdot 48.5\ \text{MPa} = 63.0\ \text{MPa}$.

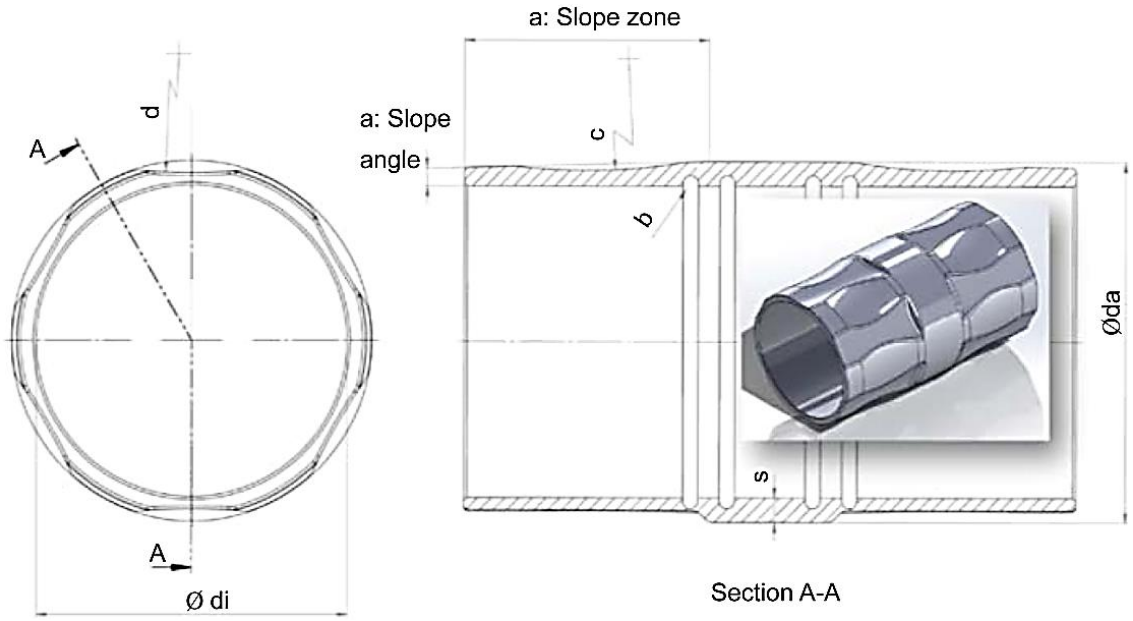

Figure 7. Swaging ring design

The reasons for the design features corresponding to the requirements of the ring and marked from *a* to *d* in Figure 7 are listed below:

a) As shown in Figure 4, the deformation of the pipe is greater in the center and gets parabolically reduced on either sides of the ring. Accordingly, the highest tensions in the inner pipe is in the region corresponding to the bottom of the ring edge and not in the central region. Considering a homogeneous tension ensures the plastic deformation to be homogenized, which requires a more useful swaging ring. In this regard, a very small slope (<1.5°) is given on the outer surface of the ring.

b) A circumferential groove is opened for the inner diameter of the ring for two sealing elements (O-Ring) in each leakage direction.

c) In the axial direction, a circumferential groove is formed in the middle of the pressure zone of the ring which prevents the pipe from getting out of the ring. When the ring is tightened, a similar plastic deformation occurs in the inner pipe, hindering the movement of the inner pipe in the axial direction.

d) The circumference of the ring's printing area is designed not to be circular, but rather wavy, to prevent the pipe from slipping out of the ring in the direction of circumferential rotation. When the ring is tightened, a similar plastic deformation occurs in the inner pipe and the inner bar is prevented from rotating inside the ring.

The design features of the swaging ring are shown as 3D in Figure 7 and are described above. Analyzes of these different design features are numerically performed using FEM.

3. Solution and Interpretation of FEM-Models

The flat swaging ring described in Figure 7 and the other swaging rings designated as A to C are designed in 3D. The 3D Models are transferred to the numerical solver program using FEM and analyzed by adding suitable physical parameters. In this study, FEM based analyzes were performed by considering four different geometric changes of the swaging ring. They possess the following geometric design features, as shown in Figure 7,

- Model “Flat” swaging ring;
- In Model “A,” small curved swaging ring;
- In Model “B,” small curved swaging ring with internal groove for sealing;
- In Model “C,” small curved, axially wavy swaging ring with internal groove for sealing.

FEM Model of four different ring designs are shown in Figure 8 (Mesh).

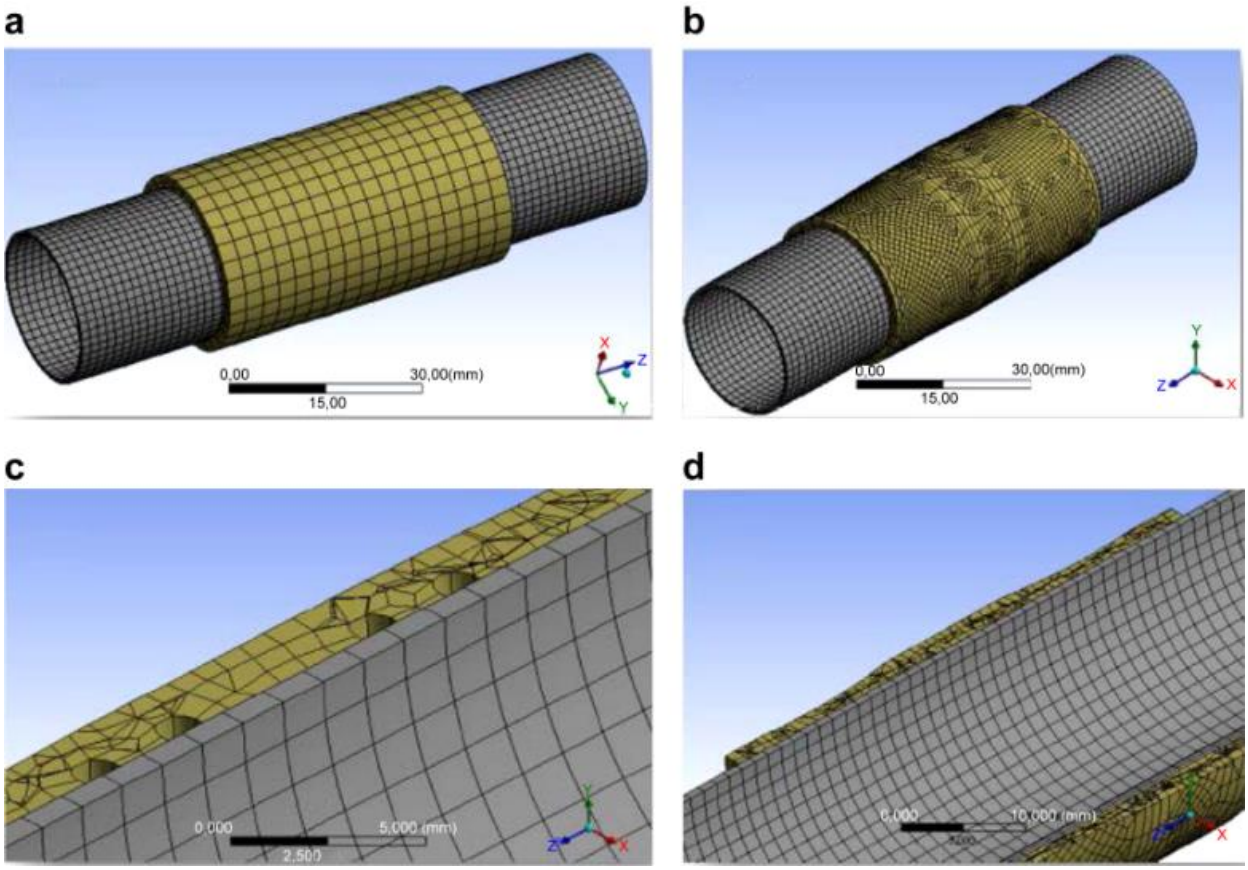

Figure 8. FEM Model of the swaging ring design (Mesh); a) Flat; b) Curved "A"; c) Curved and grooved "B"; d) Curved, grooved and wavy "C"

Figure 8 shows three separate stepwise loading cases applied in all of the FEM-Models in Simulation.

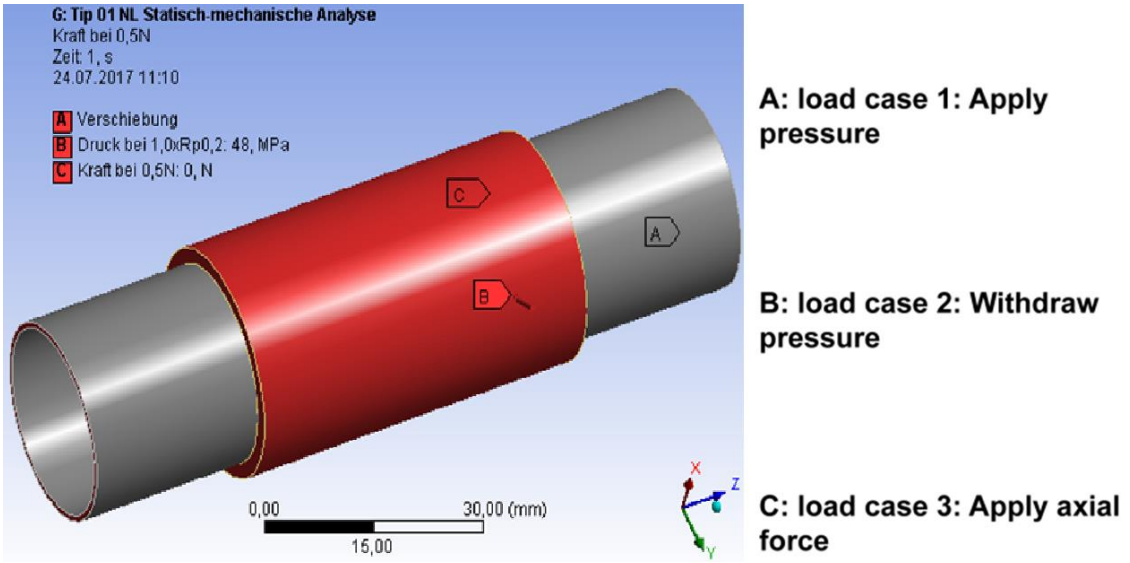

Figure 9. Load cases applied (LC: Load Case)

FEM-models are solved numerically as elastic-plastic deformation by non-linear method. In Figure 9, the deformation values of these solutions are displayed for the three loading cases explained earlier. In particular, the high percentage of plastic deformation and its homogeneous nature indicate the quality of the connection.

In the "Flat" model, shown in Figure 10, the plastic deformation is not observed to be trailing behind when the flat swaging ring is released after being subjected to elastic-plastic deformation under pressure. Hence, it is easily released under axial load. The plastic deformation component corresponds to approximately 12% of the total deflection. The pressure deformation in the inner pipe is also noticed to be very low.

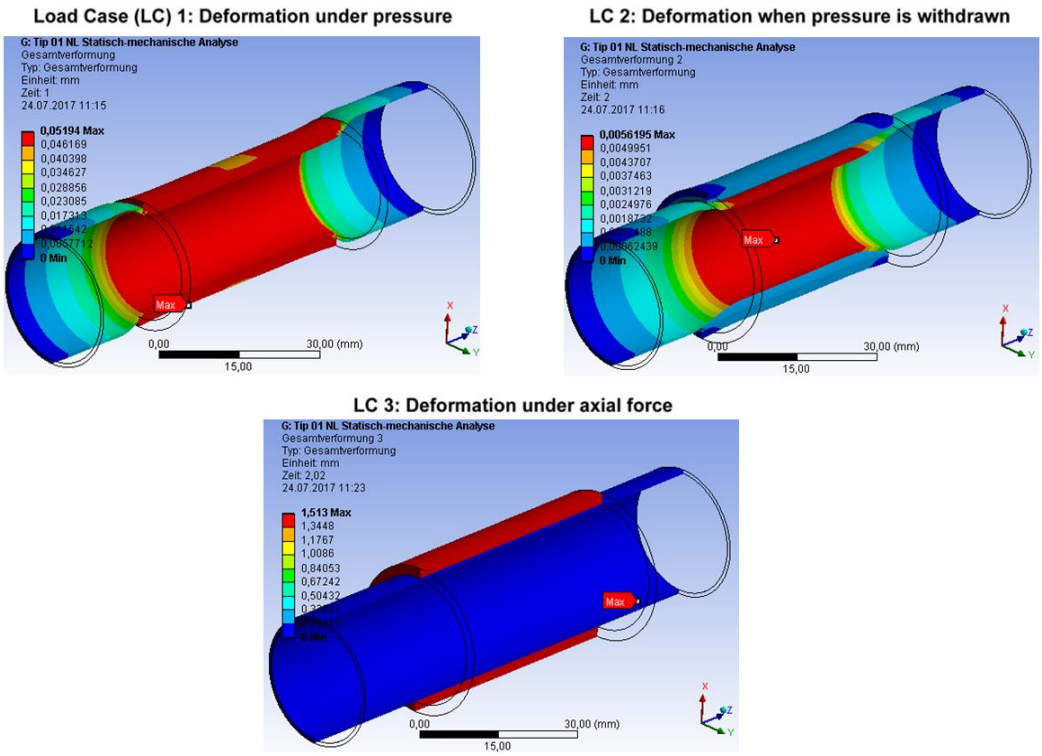

Figure 10. Flat Ring Model FEM Elastic-plastic deformations as solution results

In Model "A" in Figure 11, the plastic deformation is noticed to be lagging behind when the small curved flat swaging ring is released after being subjected to elastic-plastic deformation upon the application of pressure. Therefore, it is difficult to release under axial load. Plastic deflection corresponds to approximately 39% of the total deflection. Plastic deformation shows a variation in density and is non-homogeneous.

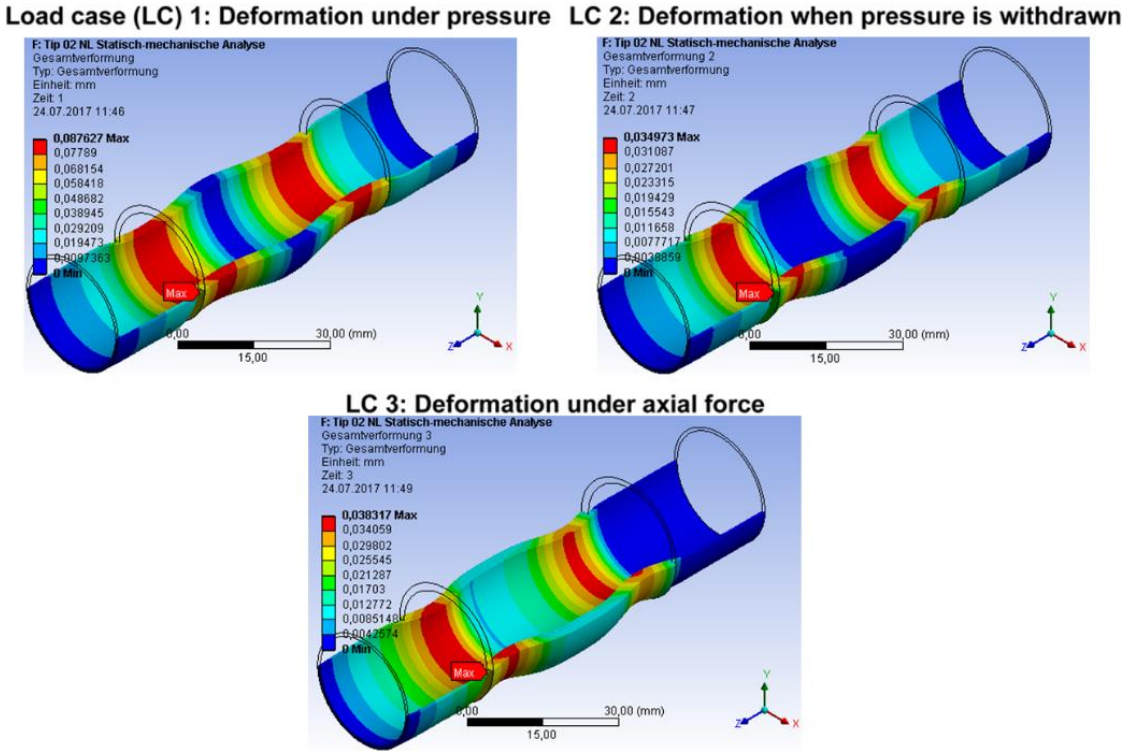

Figure 11. Elastic-plastic deformations as Model "A" FEM Solution Results

In Model "B" as shown in Figure 12, under the application of pressure, the plastic deformation is noticed to be lagging behind when the small curved flat swaging ring with internal groove for sealing is released after being subjected to elastic-plastic deformation. It now reveals difficulty to get released under axial load. The plastic

deflection component corresponds to approximately 17% of the total deflection and it is noticed to be distributed in a more homogeneous fashion as compared to Model "A", but has a lower percentage.

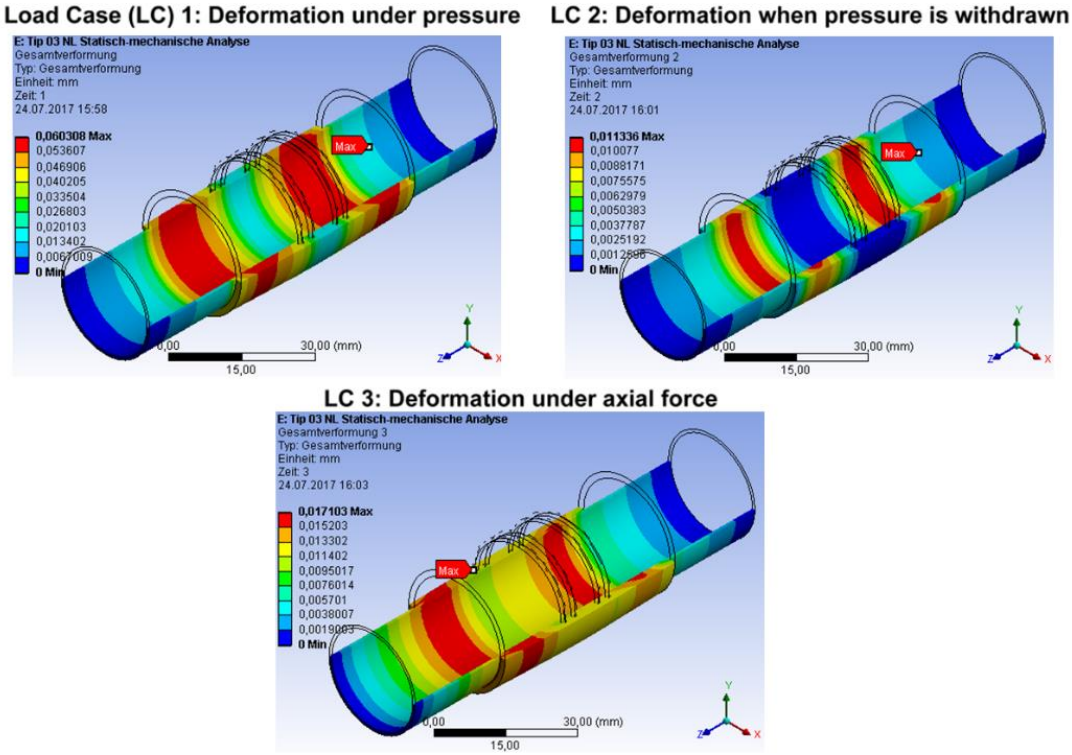

Figure 12. Elastic-plastic deformations as Model "B" FEM Solution Results

As displayed in Figure 13, Model "C" shows a lag in the plastic deformation when the small curved, axially wavy flat swaging ring with internal groove for sealing is released after being subjected to elastic-plastic deformation under pressure. In this model, the difficulty in getting released under axial load is observed. Plastic deflection contribution corresponds to approximately 78% of the total deflection. In this model, plastic deflection is both high and in the most homogeneous state. The deflection in the connected pipes is within the elastic limits. Hence, this connection is regarded as a very good theoretical solution based on both sealing and strength aspects.

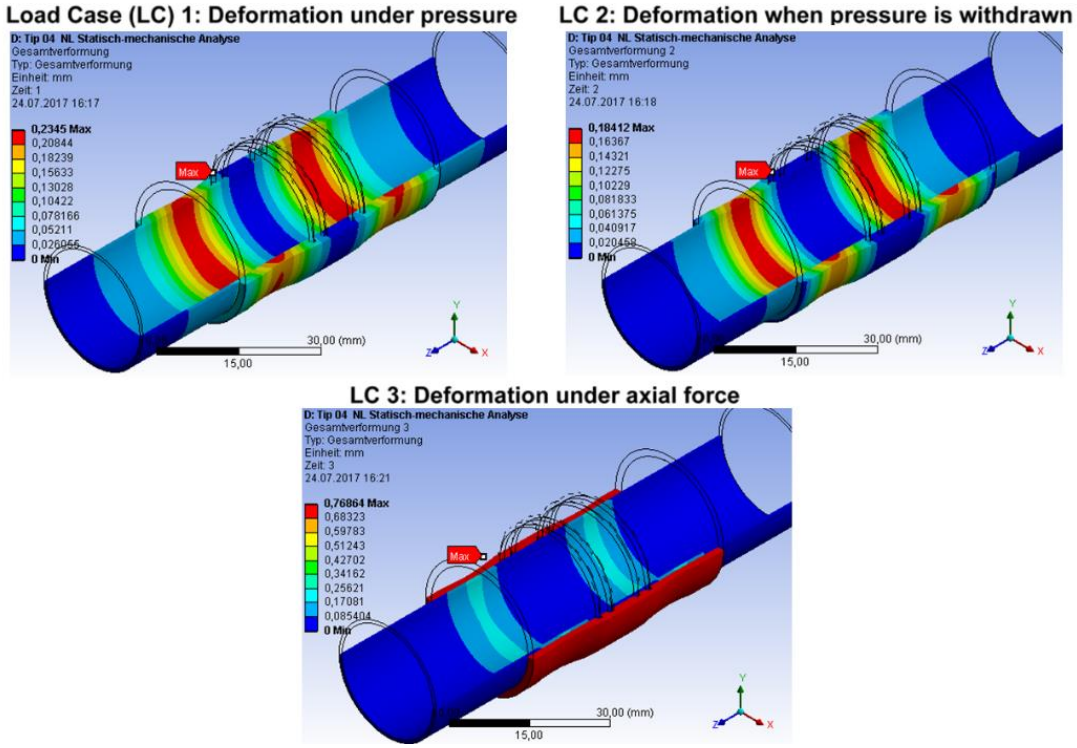

Figure 13. Elastic-plastic deformations as Model "C" FEM Solution Results.

4. Conclusion

Swaging rings play a crucial role on the reliability and efficiency of connections between pipes in engineering structures. In this study, using finite element methods and by varying the critical parameters, three different models have been built. The effect of the swaging ring design on the tightened fittings has been determined. It has been proven that these components have a great effect on the swaging force besides the parameters such as materials, mechanical properties, environmental conditions, swaging method and swaging ring materials. This study shows that among the different models compared, the most and homogeneous swaging occurs in the Model type "C" clamping ring design which comprises of small curved, axially wavy swaging ring with internal groove for sealing. Although it is possible to combine different materials and combine two different geometries with different methods, it has been shown in this study that the combinations need to be modeled and analyzed by advanced engineering since they are subject to thermal and mechanical loads in terms of usage environments and have high sealing requirements.

5. Declarations

5.1. Data Availability Statement

The data presented in this study are available on request from the corresponding author.

5.2. Acknowledgements

I would like to thank my friend Osman Akgun, doctorate student at Gazi University for supporting to this study.

5.3. Conflicts of Interest

The authors declare no conflict of interest.

6. References

[1] Bouatia, Mohammed, Rafik Demagh, and Zohra Derriche. "Structural Behavior of Pipelines Buried in Expansive Soils under Rainfall Infiltration (Part I: Transverse Behavior)." Civil Engineering Journal 6, no. 9 (September 1, 2020): 1822–1838. doi:10.28991/cej-2020-03091585.

[2] Robert, D. J., K. Soga, and T. D. O'Rourke. "Pipelines Subjected to Fault Movement in Dry and Unsaturated Soils." International Journal of Geomechanics 16, no. 5 (October 2016). doi:10.1061/(asce)gm.1943-5622.0000548.

[3] Mazina, Z R, S Zh Seysenov, S Sh Abyzgildina, and R R Tlyasheva. "Ensuring Safe Operation of the Piping Connection of Apparatus Column Type." Journal of Physics: Conference Series 1515 (April 2020): 042041. doi:10.1088/1742-6596/1515/4/042041.

[4] Adams, G.G., and M. Nosonovsky. "Contact Modeling — Forces." Tribology International 33, no. 5–6 (May 2000): 431–442. doi:10.1016/s0301-679x(00)00063-3.

[5] efunda engineering fundamentals, Applications pressure vessels, Available online: https://www.efunda.com/formulae/solid_mechanics/mat_mechanics/pressure_vessel.cfm (accessed on July 2020).

[6] Raupp, Daniela, and Karl-Heinz Wehking. "Swaged Fittings Under Tension and Fatigue Loads." Structural Engineering International 20, no. 3 (August 2010): 284–290. doi:10.2749/101686610792016808.

[7] Atak, Ahmet. "Experimental Determination and Numerical Modeling of the Stiffness of a Fastener." Materials Testing 62, no. 12 (December 7, 2020): 1215–1220. doi:10.3139/120.111607.

[8] Al-Khazaali, Mohammed, and Sai K. Vanapalli. "A Novel Experimental Technique to Investigate Soil–Pipeline Interaction Under Axial Loading in Saturated and Unsaturated Sands." Geotechnical Testing Journal 43, no. 1 (March 15, 2019): 20180059. doi:10.1520/gtj20180059.

[9] Liu, Y., M. Herrmann, C. Schenck, and B. Kuhfuss. "Plastic Deformation Components in Mandrel Free Infeed Rotary Swaging of Tubes." Procedia Manufacturing 27 (2019): 33–38. doi:10.1016/j.promfg.2018.12.040.

[10] Parker Hannifin, "Alternatives to Conventional Welded Pipe Systems", Power Engineering International, (2016), Available online: https://krishnaninc.com/technical-article-writing-pr-for-the-energy-industry-alternatives-to-conventional-welded-pipe-systems (accessed on July 2020).

[11] Zhang, Qi, Kaiqiang Jin, Dong Mu, Yisheng Zhang, and Yongyi Li. "Energy-Controlled Rotary Swaging Process for Tube Workpiece." The International Journal of Advanced Manufacturing Technology 80, no. 9–12 (May 1, 2015): 2015–2026. doi:10.1007/s00170-015-7054-x.

[12] Zhang, Qi, Kaiqiang Jin, Dong mu, Pengju Ma, and Jie Tian. "Rotary Swaging Forming Process of Tube Workpieces." Procedia Engineering 81 (2014): 2336–2341. doi:10.1016/j.proeng.2014.10.330.

[13] FENN HomeBlog, "Swaging Machines: What They Are and How They Work", Available online: https://www.fenn-torin.com/blog/how-swaging-machines-work/ (accessed on July 2020).

[14] Zhou, D., T. Sriskandarajah, M. Bamane, P. Tews, and S. Dugat. "Developing Weld Defect Acceptance Criteria for a Swaged Pipe-in-Pipe System." Offshore Technology Conference (2018). doi:10.4043/29019-ms.

[15] Pyplok Fittings Company, "A Tube Mac Manufactured Product, Introduction Part, (2020):1-6. Available online: https://pyplok.com/index.php?option=com_content&view=article&id=98&Itemid=282&lang=en (accessed on July 2020).

[16] Zhang, Qi, Kaiqiang Jin, and Dong Mu. "Tube/tube Joining Technology by Using Rotary Swaging Forming Method." Journal of Materials Processing Technology 214, no. 10 (October 2014): 2085–2094. doi:10.1016/j.jmatprotec.2014.02.002.

[17] Mali J. B., Rane S. B. and others, "Modelling and Finite Element Analysis of Double Ferrule Fit ting", Journal IJTARME, 5(1), (2016):83-87. Available online: http://www.irdindia.in/journal_ijtarme/pdf/vol5_sp_no1/16.pdf (accessed on July 2020).

[18] Greenwood, J.A. "Analysis of Elliptical Hertzian Contacts." Tribology International 30, no. 3 (March 1997): 235–237. doi:10.1016/s0301-679x(96)00051-5.

[19] Karpenko, Yu.A., and Adnan Akay. "A Numerical Model of Friction between Rough Surfaces." Tribology International 34, no. 8 (August 2001): 531–545. doi:10.1016/s0301-679x(01)00044-5.